Solar Energy 244 (2022) 126–133

Contents lists available at ScienceDirect

Solar Energy

journal homepage: www.elsevier.com/locate/solener

# Assessment on the variation of temperature coefficients of photovoltaic modules with solar irradiance

Fabiano Perin Gasparin *, Felipe Detzel Kipper, Fernando Schuck de Oliveira, Arno Krenzinger

*Federal University of Rio Grande do Sul – Solar Energy Laboratory (LABSOL), Av. Bento Gonçalves, 9500/42712. Porto Alegre – RS, Brasil. CEP 91509-910, Brazil*

ARTICLE INFO

*Keywords:*
Photovoltaics
Temperature Coefficient
PV modules

ABSTRACT

In PV system performance models, the change in temperature coefficients (TC) as a function of solar irradiance ($G$) is usually not calculated. Although the variation of the TC of open circuit voltage ($V_{oc}$) with $G$ is predicted by solar cell theory, most performance models do not account for this behavior. Equations describing the variation of TCs with $G$ are not readily available. The main objective of this paper is to experimentally evaluate the variation of TCs with $G$ of crystalline silicon PV modules. Several I-V curves were measured, with $G$ ranging from 100 to 1000 W/m$^2$ and module temperature ranging from 25 to 65 °C. A matrix of 50 I-V curves was obtained for each PV module and TCs were calculated for different $G$ values. The TC of the short-circuit current ($I_{sc}$) is practically constant with $G$, except for two studied half-cell PV modules. The absolute value of TC of maximum power ($P_m$) increases for lower irradiance values for most modules tested, but this trend is not seen for two recently manufactured PV modules where a negligible variation with $G$ was obtained. The main result is a new logarithmic function that fits the experimental data and shows a well-defined increase in the modulus of the TC of $V_{oc}$ for low irradiance values. The equation proposed to describe this behavior is a novelty to improve PV device modeling. The results presented here contribute to a better understanding of TCs under varying irradiance, an important aspect of PV module performance.

## 1. Introduction

Systems based on photovoltaic (PV) conversion of solar energy have developed rapidly in the last two decades. Power generation by PV systems is intermittent, as the power output depends mainly on the incident solar irradiance ($G$) on the plane of the PV modules. The second important variable is the temperature of the PV modules, as the power output decreases as the temperature increases. These characteristics of PV systems lead to the need for accurate models to predict the energy output based on historical meteorological data and also to monitor system performance during operation.

There are several PV performance models that vary in complexity. In some cases, even the simplest maximum power model with three independent parameters (solar irradiance, maximum power temperature coefficient and PV module temperature) is sufficient for engineering practice (de la Parra et al., 2017). However, physical models with detailed formulations can accurately calculate the entire current–voltage (I − V) curve of PV modules and arrays. This aspect is important for real-time comparison between the measured and modeled performance indicators of PV systems. Several approaches for modeling PV systems have been described in the literature, and the single diode model is usually the most studied and applied. For example, the implementation of the single diode model proposed by De Soto et al. (2006), among several other aspects, represents a trade-off between accuracy and simplicity. Other authors have presented alternative approaches to solve the single diode model (Lo Brano et al., 2010; Orioli and Di Gangi, 2013; Villalva et al., 2009), all of which have in common a physical model as a basis and different solution approaches that improve accuracy or simplicity depending on the specific implementation.

Modeling PV systems based on physical principles is the benchmark for estimating PV system yield. For example, commercial software such as PVSYST© and PVSOL©, which are available for PV system design, use physical models for the PV module. They also incorporate many variables and parameters, including shading analysis and economic models. NREL (National Renewable Energy Laboratory from the US) developed a computer program called SAM (System Advisor Model) that calculates performance models for various renewable energy sources. For PV systems, there is a simplified model called PVWATTS and a detailed one

* Corresponding author.
*E-mail addresses:* gasparin.fabiano@gmail.com, fabiano.gasparin@ufrgs.br (F. Perin Gasparin), felipedkipper@gmail.com (F. Detzel Kipper), fernandoschuck@hotmail.com (F. Schuck de Oliveira), arno.krenzinger@ufrgs.br (A. Krenzinger).

https://doi.org/10.1016/j.solener.2022.08.052
Received 1 April 2022; Received in revised form 16 August 2022; Accepted 19 August 2022
Available online 26 August 2022

based on the single diode equation.

Most PV performance models use the five-parameter single diode model to simulate the behavior of PV modules. The performance models typically have a database of multiple PV modules, including parameters from the manufacturer's data sheet measured under Standard Test Conditions (STC). Key parameters include maximum power ($P_m$), open-circuit voltage ($V_{oc}$), short-circuit current ($I_{sc}$), maximum power current ($I_{mp}$), maximum power voltage ($V_{mp}$), and fill factor (FF). Other specifications such as efficiency (η), operating conditions, system voltage, and so on are also given. There are also efforts to optimize the way to obtain the 5 parameters for the single diode model only from PV manufacturer's basic data (De Soto et al., 2006; Ishaque et al., 2011; Lo Brano et al., 2010; Orioli and Di Gangi, 2013).

The I-V curve parameters from PV modules have temperature coefficients (TCs) that represent their variation with temperature. They are necessary for the simulation of the PV system under different operating conditions. In general, TCs are determined at solar irradiance ($G$) of 1000 W/m$^2$ with spectral distribution AM 1.5. The international standard IEC 60891 states temperature spam of at least 30 °C for the TC measurement, where a range from 25 °C to 65 °C is usual.

The variation of $I_{sc}$ with temperature is usually expressed as α, and for crystalline silicon (c-Si) it is about 0.05 % °C$^{-1}$ (Osterwald et al., 1987; Paudyal and Imenes, 2021). The variation of $V_{oc}$ with temperature is reported here as β when it is an absolute value in V/°C and $\beta_{rel}$ when it is a relative value of $V_{oc}$. The value of β is important for evaluating the performance of PV systems because it significantly reduces the voltage generated by the PV modules. It was reported some time ago (Green et al., 1982) that the temperature sensitivity of $V_{oc}$ improves along with $V_{oc}$. Cells with higher $V_{oc}$ have a lower absolute value of β. Looking at some data sheets from PV module manufacturers, $\beta_{rel}$ is about − 0.35 % °C$^{-1}$ when considering earlier conventional c-Si solar cells. Currently, $\beta_{rel}$ can reach − 0.25 % °C$^{-1}$ for modern half-cell monocrystalline silicon PV modules. Table 2 in Section 3 provides the nominal TC values of the PV modules studied in this work. Data sheets from the major PV module manufacturers also indicate that the variation of $P_m$ with temperature, denoted here as $\gamma_{rel}$, is about − 0,45 % °C$^{-1}$ for earlier PV modules and can reach − 0,35 % °C$^{-1}$ for more efficient and newer c-Si PV modules.

The manufacturer's data sheets only give TCs determined from measurements of I-V curves with an irradiance of 1000 W/m$^2$. In addition, TCs are generally considered constant in the PV performance models. However, analysis of the $V_{oc}$ dependence on temperature shows that β depends on the $V_{oc}$ value and consequently on the solar irradiance. Previous work can be found in the literature that investigated the TC of $V_{oc}$ dependence on irradiance. However, there is a knowledge gap in this area as no simple equation describing this behavior is available to date. If there were a mathematical description of this physical effect, it could be used in PV performance models for engineering applications.

Dash and Gupta (2015) presented TCs measurements of different types of PV cell technologies at several irradiances and concluded that TCs are not constant over the usual operating irradiance range. However, they did not propose a mathematical relationship for this variation. A review of thermal models for PV module performance presented by Skoplaki and Palyvos (2009) evaluated the behavior of TCs but did not address the variation of β with irradiance. Berthod et al. (2016) present results on β as a function of irradiance, focusing on differences between silicon cells with doping compensation. Although the plots presented by the authors look like a logarithm function, a mathematical relationship of this dependence is not formulated or derived to be used directly in an engineering PV performance model.

Dubey et al. (2015) presented values of β measured from irradiance in the range of 600 W/m$^2$ to 1000 W/m$^2$ and found that variation of β with irradiance was not detectable for this range. However, the range of the presented measurements is relatively small considering the logarithmic aspect of the β-variation curve with irradiance. Therefore, this issue should be better investigated at irradiances below 600 W/m$^2$.

Dupré et al. (2015) observed that β decreases with the increase of $V_{oc}$, and this is because the $V_{oc}$ of the cell is a good indicator of the balance of generation and recombination of electron-hole pairs. One way to increase this balance is to concentrate the light on the cell surface, which reduces the temperature sensitivity and causes an increase in the $V_{oc}$. In other words, the higher the irradiance, the lower the absolute value or modulus of β.

The behavior of PV cells considering the variation of β with $V_{oc}$ and consequently with irradiance is described in the physical models of solar cells. However, this effect does not appear in models based on the equivalent circuit of the photovoltaic cell, the so-called five-parameter single diode model. By implementing this effect, the PV model can be improved to a more accurate representation of the actual PV module behavior. The impact of this implementation will be more noticeable at higher operating temperatures and lower irradiance. Although these conditions are not the most common in operation, finding a model that can accurately represent this behavior of PV modules while maintaining some simplicity will contribute to scientific progress in this field.

In this paper, the variation of TCs of PV modules with irradiance will

**Table 1**
Characteristics of the PV modules tested. The parameters are given in STC from the manufacturer's data sheet.

| Mod | PV device model (cell material) | # cells | $P_m$ (W) | $\eta$ *(mod)* (%) | $\eta$ *(cell)* (%) | $V_{oc}$ (V) | $V_{oc,cell}$ (V) | $I_{sc}$ (A) |
|---|---|---|---|---|---|---|---|---|
| A | WSMD-400 (m-Si PERC) | 144 (half cell) | 400 | 19.86 | 22.04 | 49.39 | 0.685 | 10.42 |
| B | GCL-M3/72H-400 (m-Si PERC) | 144 (half cell) | 400 | 19.90 | 22.25 | 48.93 | 0.679 | 10.36 |
| C | S19_290 (m-Si) | 60 | 290 | 17.6 | 19.8 | 39.30 | 0.655 | 9.80 |
| D | YL245P-29b (p-Si) | 60 | 245 | 15.0 | 16.8 | 37.8 | 0.630 | 8.63 |
| E | JKM315PP-72 315 (p-Si) | 72 | 315 | 16.23 | 17.97 | 46.2 | 0.641 | 9.01 |
| F | CSP6P-260MM (m-Si) | 60 | 260 | 16.16 | 17.80 | 37.8 | 0.630 | 8.99 |
| G | CS6P-265MM (m-Si) | 60 | 265 | 16.47 | 18.14 | 37.9 | 0.631 | 9.11 |
| H | Iso I-100 (m-Si) | 72 | 100 | 11.67 | 13.09 | 43.2 | 0.600 | 3.27 |

be studied using a series of I-V curve measurements. The main objective is to find a general relationship between the dependence of TCs and irradiance based on experimental data. The empirical relationships could be directly used for PV module performance modeling. The improved model would accurately reflect the behavior of PV modules over a wide range of operating conditions. The study will provide new insights into the behavior of the I-V curve of PV modules at different temperatures and irradiances.

The paper is organized as follows: Section 2 reviews the literature and basic theory. Section 3 describes the experimental methods used to obtain the matrix of I-V curves to determine TCs for different irradiances. Section 4 presents and discusses the results. Section 5 contains the conclusions of the paper.

## 2. Temperature coefficients of PV modules

A suitable way to determine a TC is to normalize the variation of a generic variable $Z$ as a function of temperature $T$, calculated by Eq. (1) (Emery et al., 1996).

$$TC\left(^{\circ}C^{-1}\right) = \frac{1}{Z}\frac{\partial Z}{\partial T}|_{T_{n=25^{\circ}C}} \tag{1}$$

where $T_n$ is the temperature of normalization.

As is well known, the increase in temperature leads to an increase in $I_{sc}$. The value of α, where Z in Eq. (1) stands for $I_{sc}$, is positive, i.e., $I_{sc}$ increases slightly with temperature as the energy bandgap of PV devices decreases at higher temperatures and the band-to-band absorption coefficient also increases (Green, 2003). The measurements performed in this work will help to investigate whether a variation of α is measurable or well defined as the irradiance changes.

The $V_{oc}$ decreases with temperature due to the temperature dependence of the reverse saturation current ($I_0$). The main temperature effect on $I_0$ is related to the intrinsic carrier concentration. This parameter depends on the band gap energy (lower band gaps results in higher intrinsic carrier concentration) and the energy of the carriers (higher temperature results in higher intrinsic carrier concentration). The value of $\beta_{rel}$, with $Z = V_{oc}$ in Eq. (1), is negative as mentioned earlier. Green et al. (1982) presented an aspect that was not generally recognized, namely, that the increase in $V_{oc}$ causes a decrease in the sensitivity of $V_{oc}$ to temperature. The equation supporting this behavior was also presented by Dupré et al., 2015 and is reproduced in Eq. (2).

$$\beta = \frac{dV_{oc}}{dT} = -\frac{\frac{E_{g0}}{q} - V_{oc} + \frac{\Gamma kT}{q}}{T} \tag{2}$$

where, $E_{g0}$ is the material band gap linearly extrapolated to 0 K, which for silicon is 1.206 eV (Green et al., 1982), $q$ is the elementary charge, $k$ is Boltzmann's constant, $T$ is the absolute temperature and Γ is about 3 for silicon PV cells and is used instead of 3 to account for possible temperature dependencies of other material parameters.

Eq. (2) shows that the temperature sensitivity of a photovoltaic cell depends on the $V_{oc}$ value itself. The higher the $V_{oc}$ value, the less the cell is affected by temperature. For practical purposes of PV performance modeling, a constant linear variation of $V_{oc}$ within the temperature range of the PV module over the irradiance range of operation is usually considered in PV performance models.

The TC of voltage across the I-V curve was also innovatively discussed by (Hishikawa et al., 2018) who analyzed the TC as a function of output voltage using a simple equation. Taking $V_{oc}$ as the voltage of interest in the equation presented in Hishikawa et al. (2018) we obtain Eq. (3), which is another way to express β.

$$\beta = \frac{dV_{oc}}{dT} = \frac{1}{T}\left(V_{oc} - \frac{nE_{g0}}{q}\right) \tag{3}$$

To assess the general behavior of $V_{oc}$ as a function of irradiance, we recall Eq. (4), which represents the single diode model of an ideal PV cell in which the series resistance ($R_s$) is zero and the shunt resistance ($R_{sh}$) is infinite.

$$I = I_L - I_0\left[exp\left(\frac{qV}{nkT}\right) - 1\right] \tag{4}$$

where $I$ is the current of a solar cell, $I_L$ is the light-generated current, $I_0$ is the reverse saturation current, $n$ is the diode ideality factor, and $V$ is the voltage across the terminals of the PV cell.

Substituting $I = 0$ and $V = V_{oc}$ into Eq. (4) and then isolating $V_{oc}$, yields Eq. (5) in which $V_{oc}$ depends explicitly on the logarithm of the light-generated current ($I_L$). Since $I_L$ is proportional to solar irradiance, we can conclude that $V_{oc}$ has a logarithmic dependence on irradiance.

$$V_{oc} = \frac{nkT}{q}\ln\left(\frac{I_L}{I_0} + 1\right) \tag{5}$$

Considering $G^*$ as the normalized solar irradiance, where $G^* = 1$ for 1000 W/m$^2$, Eq. (6) gives an expression for an ideal solar cell relating $V_{oc}$ to G* and showing the explicit logarithmic dependence of $V_{oc}$ on $G$.

$$V_{oc}(G^*) = V_{oc\_STC} + \frac{nkT}{q}\ln G^* \tag{6}$$

where $V_{oc}$(G*) is the open-circuit voltage at $G^*$, and $V_{oc\_STC}$ is the $V_{oc}$ at STC.

In the experimental work presented by Cotfas et al. (2018), a variation of β with solar irradiance is shown. However, their measurements were performed only up to the smallest value of 400 W/m$^2$. In this case, the logarithmic function was not clear and a linear function was fitted to the experimental values.

If β is not constant over solar irradiance according to the theoretical model, it should be a simple matter to implement this variation in the five-parameter single diode model represented by Eq. (7). An easy way to implement the variation of β with solar irradiance is to solve Eq. (7) for open-circuit conditions with $V = V_{oc}$ and $I = 0$.

$$I = I_L - I_0\left[exp\left(\frac{q(V + IR_s)}{N_s nkT}\right) - 1\right] - \frac{V + IR_s}{R_P} \tag{7}$$

Isolating $I_0$ from Eq. (7) under open-circuit conditions leads to Eq. (8), which calculates the new values of $I_o$ corrected for temperature and irradiance. A similar method is used by Villalva et al. (2009) to reproduce the I-V curve in different conditions, but so far no adjustments of β have been considered.

$$I_0 = \frac{I_L - \frac{V_{oc}}{R_p}}{exp\left(\frac{qV_{oc}}{N_s nkT}\right) - 1} \tag{8}$$

where $N_s$ is the number of PV cells connected in series in a PV module.

The effect of a β corrected for irradiance can be determined using Eq. (9) for each irradiance condition and considering β as a function of irradiance.

$$V_{OC2} = V_{OC1} + \beta(G)(T_2 - T_1) \tag{9}$$

where $V_{oc2}$ is the value for the new condition, $T_2$ is the temperature in the new condition, $V_{oc1}$ is normally $V_{oc}$ at STC, $T_1$ is normally 25° C and β(G) is the TC of $V_{oc}$ corrected for irradiance.

After reviewing some basic aspects of the behavior of $V_{oc}$ and the relationship with temperature and irradiance, the methodology proposed in the next section has the main objective of checking the parameters ($V_{oc}$, $I_{sc}$ and $P_m$) under different irradiance and temperature conditions to obtain the general behavior of the TCs of PV modules under different conditions.

## 3. Methodology

A set of eight commercial c-Si PV modules listed in Table 1 were

**Table 2**
Nominal temperature coefficients from the data sheets of the evaluated PV modules.

| PV Module | α [%/°C] | $\beta_{rel}$ [%/°C] | $\gamma_{rel}$ [%/°C] |
|---|---|---|---|
| A | 0.05 | −0.27 | −0.37 |
| B | 0.06 | −0.30 | −0.39 |
| C | 0.05 | −0.29 | −0.40 |
| D | 0.05 | −0.32 | −0.42 |
| E | 0.06 | −0.31 | −0.41 |
| F | 0.06 | −0.35 | −0.45 |
| G | 0.06 | −0.35 | −0.45 |
| H | not informed | | |

evaluated in this work. These are monocrystalline (m-Si) and polycrystalline (p-Si) silicon PV modules. The selection process attempted to consider PV modules with different nominal efficiencies and a considerable range of $V_{oc}$ per cell ($V_{oc,cell}$). Cells efficiencies are also listed in Table 1. There are approximately 20 years of manufacturing time between the lowest efficiency PV module (Module H) manufactured around 2002–2003 and the PV modules manufactured in 2021 (Modules A-B). All PV modules were not previously exposed to the Sun, but they received only a light soaking of about 5–10 kWh/m$^2$.

Several *I-V* curves of the PV modules listed in Table 1 were measured in a Large Area Pulsed Solar Simulator (LAPSS) model PASAN Sunsim 3C. The I-V curve is traced from $I_{sc}$ to $V_{oc}$ in a single sweep, with 418 *I-V* pairs measured during the 10 ms flash. The I-V curves were measured with irradiances from 100 to 1000 W/m$^2$ in an interval of 100 W/m$^2$. The I-V curve for each irradiance was measured at average PV module temperatures of 25 °C, 35 °C, 45 °C, 55 °C, and 65 °C. The matrix for each PV module contains 50 I-V curves that allow the determination of TCs for each irradiance. The LAPSS is used to obtain different irradiances using mask attenuators placed in front of the light source. The irradiance is accurately controlled by the equipment via a feedback loop with the irradiance measured in the test plane. The electrical uncertainty is 0.5% and the spatial non-uniformity determined after installation is better than 0.5%.

An assessment of the spectral mismatch of this LAPSS reported by Droz et al. (2010) found it to exceed the specifications of IEA 60904–9 for a class A solar simulator. According to Fakhfouri et al. (2010), a typical spectral mismatch for m-Si and p-Si devices for this LAPSS model is about 0.1%. For a standard class A solar simulator, this mismatch could be as high as 0.96%. Since the attenuators used to reduce the irradiance are simple perforated masks that do not affect the spectral distribution of the radiation emitted by the LAPSS light source, no spectral correction was required for the measurements. Another study by Piccoli Junior et al. (2020), which analyzed the spectral distribution in the specific LAPSS of the LABSOL, showed that the correction due to spectral mismatch with respect to the standard spectrum AM 1.5 for c-Si cells is of the order of 0.04%, i.e., it can be neglected.

The PV modules are placed in a thermostatic chamber that heats them to a controlled temperature. The thermostatic chamber is installed in the test plane in the dark tunnel of the solar simulator as shown in Fig. 1.

The chamber is heated by a resistance wire inserted in alternate channels of an alveolar polycarbonate plate which becomes a heating plate. The heating plate consists of 7 resistor sections approximately 20 cm high, each section being formed by 14 turns of the wire inside the polycarbonate plate. Each resistor section emits about 400 W at 220 V, so the whole heating plate dissipates about 2800 W. The chamber has fans on the bottom and top of the PV module to perform forced convection and unify the temperature. The convection system consists of 25 fans, 14 of which are installed at the top and 11 at the bottom of the chamber. In this way, air is forced up through the back of the PV module and down through the front of the module while the doors are closed. To control the heating more efficiently in the vertical direction and improve temperature uniformity, the heating plate is divided into three heating zones with independent temperature control for each zone. Temperature control is provided by proportional-integral-derivative (PID) controllers (NOVUS N1030) and solid-state relays that supply regulated power to the heating plate. A Pt100 temperature sensor to control the temperature of each heating zone is mounted on the back of the PV module with aluminum tape.

In addition to the three sensors of the temperature control loops, nine Pt100 sensors were installed and connected to a data acquisition device (Keysight 34980A) controlled by Benchlink 34980A software. The IEC 60891 international standard (IEC 60891, 2009) specifies the procedures for determining the TCs of PV modules and recommends the installation of four temperature sensors on the back of the module. The recommendation of IEC 60891 was exceeded in the experimental setup, as the objective was also to measure the temperature at nine positions of the PV module to obtain the average temperature, as well as to verify the temperature non-uniformity at each time during the tests. The average temperature of the nine sensors was used to determine the TCs and the temperature non-uniformity was kept at ± 2 °C. For each measurement of the I-V curve, the thermostatic chamber is opened for a few seconds to expose the module to the LAPSS radiation. Immediately after the I-V curve measurement, the door is closed to keep the temperature as uniform as possible.

**Fig. 1.** Left: Thermostatic chamber in the dark tunnel of the solar simulator with the left door closed; Right: Front view of the thermostatic chamber with the doors open and a PV module inside.

TCs are determined by measuring the parameters extracted from the I-V curve at different temperatures. The data of $V_{oc}$, $I_{sc}$ and $P_m$ are plotted as a function of the average temperature of the nine Pt100 sensors and a linear regression line is used to obtain the TCs for these parameters. Then the values of α, β, and γ for each irradiance are calculated in the relative form [%/°C]. The results of TC are normalized to the value of the TC obtained with G of 1000 W/m$^2$, and thus a general relationship representing the behavior of TCs with irradiance could be evaluated or derived. Table 2 shows the nominal TCs of the PV modules studied where these values are taken from the manufacturer's data sheets.

## 4. Results and discussion

Table 3 shows the measured α results for all PV modules tested. From the values in Table 3 and the normalized results in Fig. 2, it can be seen that PV modules A, B, and G showed an increase in α at lower irradiance values. For the remaining PV modules, α increased only slightly or remained practically constant. Given the small effect of α on PV module energy performance, no attempt was made to determine an equation that would incorporate this dependence into simulation models for PV module performance. The most efficient PV modules in the set (A and B) tend to increase the value of α noticeably in the low irradiance region. This suggests that the influence of temperature is greater at lower irradiance values, which is likely due to the better performance and lower losses in the PV cells for this type of module. A deeper discussion of the variation of α with solar irradiance is beyond the scope of this article, where the variation of β with solar irradiance is discussed in more detail afterward.

Table 4 shows the measured TCs of $P_m$ ($\gamma_{rel}$) and these values are plotted in Fig. 3. The values of $\gamma_{rel}$ show a difference in the behavior of the conventional c-Si PV modules (modules from D to H) to the more efficient ones (modules A to C).

The more efficient PV modules show an almost constant $\gamma_{rel}$ over the assessed irradiance range, while older PV modules show a clear dependence on $G$. In this case, it seems impossible to obtain a single equation covering all c-Si cell technologies. Therefore, there is no suitable general equation that can be inserted in simulation models for PV module performance, especially in maximum power models that use directly $\gamma_{rel}$ from data sheets. Nonetheless, the results presented in Fig. 3 provide an important basis for future attempts to improve maximum power models that calculated power based only on linear variation with irradiance and temperature. Future research can address this behavior in more detail and help improve maximum power models where the behavior of $\gamma_{rel}$ has noticeable importance.

With all $V_{oc}$ values at different temperatures from the matrix of I-V curves, it is possible to calculate β for each irradiance. The values obtained for all PV modules tested in this work are listed in Table 5, where the absolute values of voltage reduction are given in mV/°C per cell. Table 5 is useful to compare the measured results with the typical values reported in the literature for c-Si, which are around − 2.2 mV/°C (Cotfas et al., 2018).

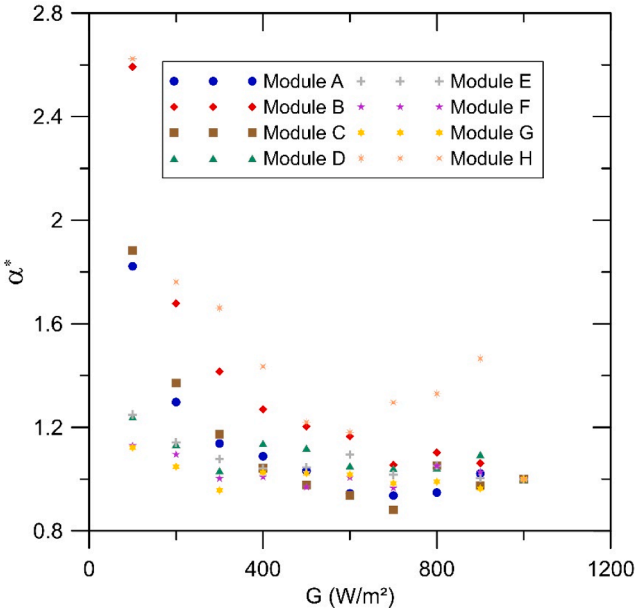


**Fig. 2.** Plot showing normalized values of α from the set of PV modules as a function of solar irradiance.

A normalized value of β for a PV cell can be determined analytically if β(G*) is normalized by β(STC), using Eq. (2) and Eq. (6), which results in Eq. (10). Eq. (6) is introduced here to account for the variation of $V_{oc}$ with $G$.

$$\beta^{**} = \frac{\beta(G^*)}{\beta(STC)} = \frac{\frac{E_{g0}}{q} - V_{oc\_STC} - \frac{nkT}{q}\ln G^* + \frac{\Gamma kT}{q}}{\frac{E_{g0}}{q} - V_{oc\_STC} + \frac{\Gamma kT}{q}} \tag{10}$$

After simplifying Eq. (10), using $k$ in eV/K, and considering $q$ as the unit of elementary charge, we obtain Eq. (11), which is a normalized value of β by its value at STC. β** indicates that $G$ is also normalized.

$$\beta^{**} = 1 - \frac{nkT\ln G^*}{E_{g0} - V_{oc\_STC} + \Gamma kT} \tag{11}$$

Eq. (11) is a useful equation to correct β with G*, but it still depends on the specific parameters of the PV module ($n$, $V_{oc\_STC}$ and Γ). An attempt to find a general relationship for a normalized β for all c-Si PV modules does not seem to be feasible in this way.

Currently, it is common to represent β as a relative value, given as a percentage of $V_{oc}$ at the normalization irradiance. In this way, $\beta_{rel}$ (%) is calculated by dividing β in V/°C by the $V_{oc}$ value at each irradiance and the PV module at 25 °C. Table 6 shows the measured values of $\beta_{rel}$ in %/°C for all PV modules evaluated.

**Table 3**
Measured TC of $I_{sc}$ under different irradiances.

| $G$ [W/m$^2$] | α [%/°C] | | | | | | | |
|---|---|---|---|---|---|---|---|---|
| | PV module | | | | | | | |
| | A | B | C | D | E | F | G | H |
| 1000 | 0.070 | 0.058 | 0.065 | 0.051 | 0.060 | 0.063 | 0.066 | 0.040 |
| 900 | 0.072 | 0.061 | 0.063 | 0.055 | 0.060 | 0.065 | 0.064 | 0.058 |
| 800 | 0.066 | 0.064 | 0.068 | 0.053 | 0.063 | 0.066 | 0.065 | 0.053 |
| 700 | 0.066 | 0.061 | 0.057 | 0.053 | 0.061 | 0.061 | 0.065 | 0.052 |
| 600 | 0.066 | 0.067 | 0.061 | 0.053 | 0.065 | 0.064 | 0.067 | 0.047 |
| 500 | 0.072 | 0.070 | 0.064 | 0.057 | 0.062 | 0.061 | 0.068 | 0.048 |
| 400 | 0.076 | 0.073 | 0.068 | 0.058 | 0.062 | 0.064 | 0.068 | 0.057 |
| 300 | 0.080 | 0.082 | 0.076 | 0.052 | 0.064 | 0.063 | 0.063 | 0.066 |
| 200 | 0.091 | 0.097 | 0.089 | 0.057 | 0.068 | 0.069 | 0.069 | 0.070 |
| 100 | 0.128 | 0.150 | 0.122 | 0.063 | 0.074 | 0.071 | 0.074 | 0.104 |

**Table 4**
Temperature coefficients of $P_m$ ($\gamma_{rel}$) determined for different irradiances.

| $G$ [W/m$^2$] | $\gamma_{rel}$ [%/°C] | | | | | | | |
|---|---|---|---|---|---|---|---|---|
| | PV module | | | | | | | |
| | A | B | C | D | E | F | G | H |
| 1000 | −0.34 | −0.34 | −0.40 | −0.44 | −0.41 | −0.42 | −0.46 | −0.46 |
| 900 | −0.34 | −0.34 | −0.41 | −0.43 | −0.42 | −0.42 | −0.44 | −0.47 |
| 800 | −0.34 | −0.34 | −0.41 | −0.44 | −0.42 | −0.43 | −0.45 | −0.48 |
| 700 | −0.35 | −0.35 | −0.40 | −0.44 | −0.42 | −0.43 | −0.45 | −0.48 |
| 600 | −0.35 | −0.34 | −0.40 | −0.44 | −0.43 | −0.43 | −0.45 | −0.48 |
| 500 | −0.35 | −0.35 | −0.40 | −0.44 | −0.44 | −0.43 | −0.46 | −0.48 |
| 400 | −0.35 | −0.35 | −0.40 | −0.44 | −0.44 | −0.44 | −0.46 | −0.48 |
| 300 | −0.35 | −0.35 | −0.39 | −0.44 | −0.45 | −0.45 | −0.47 | −0.48 |
| 200 | −0.36 | −0.35 | −0.38 | −0.45 | −0.47 | −0.46 | −0.48 | −0.48 |
| 100 | −0.36 | −0.33 | −0.38 | −0.47 | −0.49 | −0.48 | −0.50 | −0.48 |

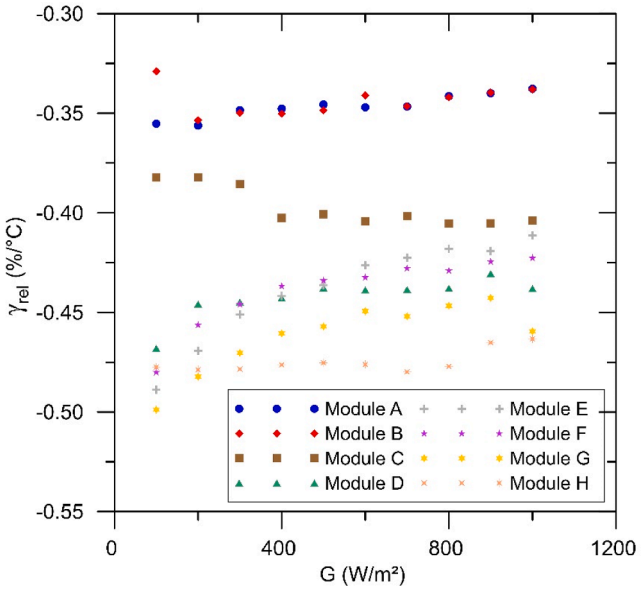


**Fig. 3.** The TC of $P_m$ ($\gamma_{rel}$) for each PV module as a function of irradiance.

Fig. 4 shows the $\beta_{rel}$ values (%/°C) for the set of eight PV modules evaluated as a function of irradiance. It can be seen from Fig. 4 that all modules show the same tendency, namely a decrease in $\beta_{rel}$ (more negative values) as G decreases. In other words, $V_{oc}$ is more sensitive to temperature at lower irradiance values. Analyzing the graph, it is noticeable that the variation of $\beta_{rel}$ with irradiance should be taken into account, because at lower irradiances the variation of $\beta_{rel}$ is more pronounced, especially at $G < 600$ W/m$^2$. In addition, more efficient half-cell PV modules (A and B) have lower absolute values of $\beta_{rel}$ (less sensitive to temperature).

The plots in Fig. 4 show that a general relationship can be established, given that the points appear to have only an offset between modules. To obtain a general relationship that calculates $\beta_{rel}$ for an arbitrary irradiance, all values of $\beta_{rel}$(%) for each PV module were normalized to the values corresponding to an irradiance of 1000 W/m$^2$ according to Eq. (12).

$$\beta_{rel}^{**} = \frac{\beta_{rel}(G^*)}{\beta_{rel}(STC)} \tag{12}$$

The experimental results of $\beta_{rel}^{**}$ are shown in Fig. 5 where the irradiance is also normalized (G*). From this plot, a general function can be derived that relates $\beta_{rel}$ at each irradiance to the value at 1000 W/m$^2$, which is usually reported by the manufacturer. The symbol $\beta_{rel}$** indicates a normalized value as a function of G*. A logarithmic function fits the grouped data very well with a coefficient of determination $R^2 > 0.95$. The analytical equation for $\beta_{rel}^{**}$ (Eq. (14)) is deducted later and is also plotted in Fig. 5 to show de equivalence between experimental results and a theoretical equation.

The equation shown in Fig. 5 derived from the curve fit on the measured data has an original linear coefficient of 1.0045. In the proposed Eq. (13), the value is rounded to 1 to keep it simple and consistent with the analytical result, where $\beta_{rel}$** = 1 for G* = 1. Eq. (13) can be implemented to adjust the value of $\beta_{rel}$ for any desired irradiance level. The only input parameter would be the irradiance and the value of $\beta_{rel}$ measured at $G = 1000$ W/m$^2$.

$$\beta_{rel}^{**} = -0.108 \ln G^* + 1 \tag{13}$$

The normalized $\beta_{rel}$ of all tested PV modules follows a well-defined logarithmic trend, regardless of PV module efficiency or individual characteristics. Eq. (13) proposed here describes the dependence of $\beta_{rel}$ on irradiance and it can be applied based on the $\beta_{rel}$ provided in the manufacturer's data sheets. The results were obtained from a set of eight

**Table 5**
Temperature coefficients of $V_{oc}$ (β) in voltage variation per cell for different irradiances.

| $G$ [W/m$^2$] | β [mV/°C cell] | | | | | | | |
|---|---|---|---|---|---|---|---|---|
| | PV module | | | | | | | |
| | A | B | C | D | E | F | G | H |
| 1000 | −1.81 | −1.81 | −1.89 | −1.99 | −2.02 | −2.04 | −2.19 | −2.13 |
| 900 | −1.85 | −1.84 | −1.92 | −1.98 | −2.06 | −2.06 | −2.14 | −2.18 |
| 800 | −1.84 | −1.86 | −1.94 | −2.03 | −2.06 | −2.08 | −2.18 | −2.22 |
| 700 | −1.88 | −1.88 | −1.93 | −2.04 | −2.07 | −2.07 | −2.20 | −2.24 |
| 600 | −1.88 | −1.86 | −1.97 | −2.06 | −2.12 | −2.10 | −2.20 | −2.24 |
| 500 | −1.88 | −1.92 | −1.99 | −2.06 | −2.14 | −2.11 | −2.24 | −2.24 |
| 400 | −1.92 | −1.94 | −2.02 | −2.10 | −2.16 | −2.14 | −2.25 | −2.26 |
| 300 | −1.92 | −1.95 | −2.02 | −2.10 | −2.20 | −2.18 | −2.29 | −2.27 |
| 200 | −1.99 | −1.99 | −2.02 | −2.11 | −2.26 | −2.22 | −2.34 | −2.28 |
| 100 | −2.10 | −2.07 | −2.12 | −2.18 | −2.32 | −2.32 | −2.42 | −2.33 |

**Table 6**
Measured temperature coefficients of $V_{oc}$ ($\beta_{rel}$) for different irradiances.

| $G$ [W/m$^2$] | $\beta_{rel}$ [%/°C] | | | | | | | |
|---|---|---|---|---|---|---|---|---|
| | PV module | | | | | | | |
| | A | B | C | D | E | F | G | H |
| 1000 | −0.27 | −0.27 | −0.29 | −0.32 | −0.32 | −0.33 | −0.35 | −0.36 |
| 900 | −0.27 | −0.28 | −0.29 | −0.32 | −0.33 | −0.33 | −0.34 | −0.37 |
| 800 | −0.27 | −0.28 | −0.30 | −0.33 | −0.33 | −0.34 | −0.35 | −0.38 |
| 700 | −0.28 | −0.28 | −0.30 | −0.33 | −0.33 | −0.34 | −0.36 | −0.39 |
| 600 | −0.28 | −0.28 | −0.31 | −0.34 | −0.34 | −0.34 | −0.36 | −0.39 |
| 500 | −0.29 | −0.30 | −0.31 | −0.34 | −0.35 | −0.35 | −0.37 | −0.39 |
| 400 | −0.30 | −0.30 | −0.32 | −0.35 | −0.36 | −0.36 | −0.37 | −0.40 |
| 300 | −0.30 | −0.31 | −0.33 | −0.36 | −0.37 | −0.37 | −0.39 | −0.41 |
| 200 | −0.32 | −0.32 | −0.33 | −0.37 | −0.39 | −0.38 | −0.40 | −0.42 |
| 100 | −0.34 | −0.34 | −0.36 | −0.39 | −0.41 | −0.42 | −0.43 | −0.45 |

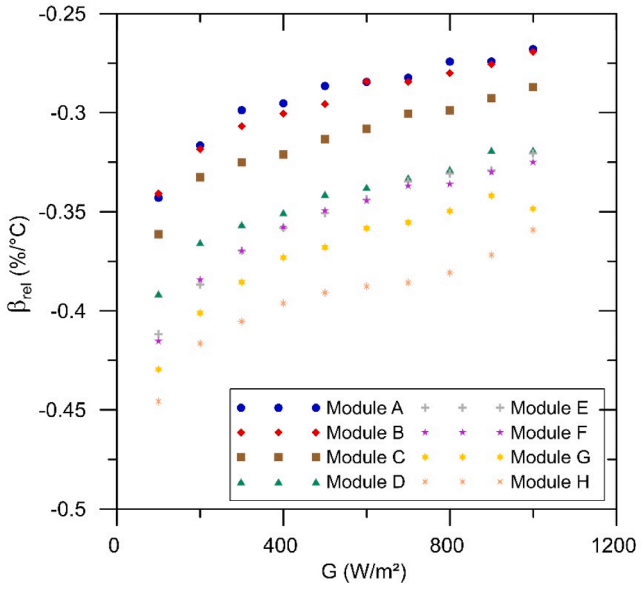


**Fig. 4.** Plots of $\beta_{rel}$ (%/°C) as a function of solar irradiance.

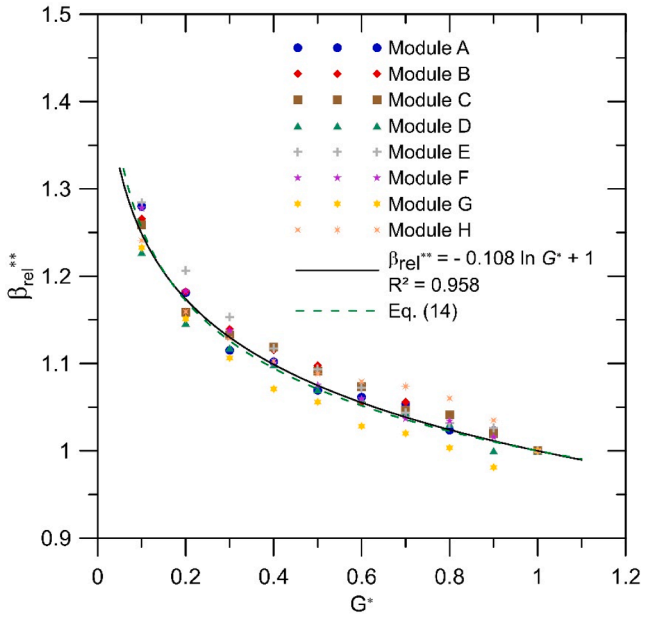


**Fig. 5.** Normalized TC of $V_{oc}$ ($\beta_{rel}$**) plotted as a function of normalized irradiance (G*) for the PV modules studied. The function fitted to the data is shown and also the deducted analytical equation for $\beta_{rel}$** (Eq. (14)).

c-Si PV modules evaluated in this work, but based on the samples evaluated so far, the proposed equation is quite independent of the manufacturer or specific parameters and could be applied to any c-Si PV module without significant error.

Eq. (13) was derived by curve fitting and the logarithmic function was chosen for convenience along with the resulting good fit. When analyzing the equations of β from solar cell theory, a logarithmic function for the $\beta_{rel}$** could be not obvious. To verify the logarithmic nature and make an attempt to obtain an analytical function, Eq. (12) is used as a starting point, i.e., the definition of $\beta_{rel}$**. After some algebraic operations, Eq. (14) can be obtained, which is an analytical expression for $\beta_{rel}$**. Eq. (14) is calculated by dividing the numerator of Eq. (10) by $V_{oc}(G^*)$ (Eq. (6)) and the denominator of Eq. (10) by $V_{oc\_STC}$. For dimensional consistency, $q$ in Eq. (14) is an elementary charge unit (q = 1) and $k$ is in units of [eV/K].

$$\beta_{rel}^{**} = \left(\frac{E_{g0} + \Gamma kT}{V_{oc\_STC} + nkT\ln G^*} - 1\right) \times \left(\frac{V_{oc\_STC}}{E_{g0} + \Gamma kT - V_{oc\_STC}}\right) \quad (14)$$

No direct analytical correspondence was found between Eq. (13) and Eq. (14). However, the logarithmic dependence of $\beta_{rel}$** with G* appears explicitly in Eq. (14). Although the analytical equivalence does not appear to be clear, numerical equivalence between Eq. (13) and Eq. (14) was found after testing numerical solutions with typical silicon parameters ($V_{oc\_STC}$ = 0.675 V, $n$ = 1.2, Γ = 3) and also using curve fitting. Eq. (14) was calculated with these typical values and is plotted in Fig. 5 to show this equivalence. The numerical equivalence has negligible dependence on the chosen $V_{oc\_STC}$. Small adjustments on $n$ and Γ in Eq. (14) can reproduce Eq. (13) very well for the PV modules. This result can also be deduced from the small scatter in Fig. 5. In this way, Eq. (13) can be used for any c-Si PV module to calculate $\beta_{rel}$** for all irradiance conditions in the PV module operating range.

## 5. Conclusions

The results obtained in this work are based on extensive experimental measurements of TCs on a set of eight commercial c-Si PV modules from different manufacturers and cell technologies. In addition, the selection of PV modules was made to cover a range of efficiencies and $V_{oc}$ per cell to obtain a representative sample of different c-Si cells.

An attempt to model the variation of the TC of $I_{sc}$ (α) with irradiance would not lead to appreciable improvement in PV device modeling. Although the measurements showed some dependence on irradiance, especially for half-cell PV modules, it does not seem reasonable to derive an expression for this behavior. Also, there was no general behavior for all modules tested in this work. The new experimental data in this work show that currently, high-efficiency modules have a practically constant TC of $P_m$ over the irradiance range of interest. Moreover, the behavior of

TC of $P_m$ is not the same for all PV modules tested. Conventional c-Si PV modules show a greater reduction in $P_m$ due to temperature at lower irradiance levels, but no clear trend can be observed for all modules studied.

An equation was presented to predict and determine the behavior of relative TC of $V_{oc}$ ($\beta_{rel}$) as a function of irradiance. The equation is based on several I-V curve measurements in a solar simulator and fits well with the results for all PV modules tested. The variation of $\beta_{rel}$ with irradiance has a logarithmic behavior, i.e., at low irradiances the variation of the parameter is quite pronounced and the $V_{oc}$ of the PV module is more sensitive to temperature. The equation obtained by fitting the data (Eq. (13)) can increase the accuracy of a PV device performance model, especially at low irradiance and high temperatures. It was also deducted an analytical equation based on the solar cells theory that is equivalent to the empirical equation obtained by curve fit.

The variation of TC of $V_{oc}$ with solar irradiance was known from previous theoretical models. However, to our knowledge, the equation proposed in this paper is reported for the first time, which is simple and describes well the variation of $\beta_{rel}$ using a logarithmic function with only two terms. The results can improve the PV accuracy of PV device modeling in a wide range of solar irradiance and temperature, including an effect not usually considered in engineering applications.

## Declaration of Competing Interest

The authors declare that they have no known competing financial interests or personal relationships that could have appeared to influence the work reported in this paper.

## Acknowledgments

This work was financially supported by CNPq – Brazil (Conselho Nacional de Desenvolvimento Científico e Tecnológico) and CAPES – Brazil (Coordenação de Aperfeiçoamento de Pessoal de Nível Superior).

## References

Berthod, C., Strandberg, R., Yordanov, G.H., Beyer, H.G., Odden, J.O., 2016. On the variability of the temperature coefficients of mc-Si solar cells with irradiance. Energy Procedia 92, 2–9. https://doi.org/10.1016/j.egypro.2016.07.002.

Cotfas, D.T., Cotfas, P.A., Machidon, O.M., 2018. Study of temperature coefficients for parameters of photovoltaic cells. Int. J. Photoenergy 2018, 1–12.

Dash, P.K., Gupta, N.C., 2015. Variation of temperature coefficient of different technology photovoltaic modules with respect to irradiance. Int. J. Curr. Eng. Technol. 55, 2277–4106.

de la Parra, I., Muñoz, M., Lorenzo, E., García, M., Marcos, J., Martínez-Moreno, F., 2017. PV performance modelling: A review in the light of quality assurance for large PV plants. Renew. Sustain. Energy Rev. 78, 780–797. https://doi.org/10.1016/j.rser.2017.04.080.

De Soto, W., Klein, S.A., Beckman, W.A., 2006. Improvement and validation of a model for photovoltaic array performance. Sol. Energy 80, 78–88. https://doi.org/10.1016/j.solener.2005.06.010.

Droz, C., Fakhfouri, V., Pelet, Y., Roux, J., Peguiron, N., Beljean, P.-R., 2010. Evaluation of commercial large area solar simulator: features exceeding the IEC standard class AAA. 25th Eur. Photovolt. Sol. Energy Conf. Exhib. / 5th World Conf. Photovolt. Energy Conversion, 6-10 Sept. 2010, Val. Spain 3884–3888. https://doi.org/10.4229/25thEUPVSEC2010-4CO.20.5.

Dubey, R., Batra, P., Chattopadhyay, S., Kottantharayil, A., Arora, B.M., Narasimhan, K. L., Vasi, J., 2015. Measurement of temperature coefficient of photovoltaic modules in field and comparison with laboratory measurements. 2015 IEEE 42nd Photovolt. Spec. Conf. PVSC 2015. https://doi.org/10.1109/PVSC.2015.7355852.

Dupré, O., Vaillon, R., Green, M.A., 2015. Physics of the temperature coefficients of solar cells. Sol. Energy Mater. Sol. Cells 140, 92–100. https://doi.org/10.1016/j.solmat.2015.03.025.

Emery, K., Burdick, J., Caiyem, Y., Dunlavy, D., Field, H., Kroposki, B., Moriarty, T., Ottoson, L., Rummel, S., Strand, T., Wanlass, M.W., 1996. Temperature dependence of photovoltaic cells, modules, and systems. Conf. Rec. IEEE Photovolt. Spec. Conf. 1275–1278 https://doi.org/10.1109/pvsc.1996.564365.

Fakhfouri, V., Pelet, Y., Roux, J., Droz, C., Peguiron, N., Beljean, P.-R., 2010. Proposal of a new standard for the spetral match classification of solar simulators. In: 25th European Photovoltaic Solar Energy Conference and Exhibition / 5th World Conference on Photovoltaic Energy Conversion, 6–10 September 2010. Valencia, Spain, pp. 4209–4211.

Green, M.A., 2003. General temperature dependence of solar cell performance and implications for device modelling. Prog. Photovoltaics Res. Appl. 11, 333–340. https://doi.org/10.1002/pip.496.

Green, M.A., Emery, K., Blakers, A.W., 1982. Silicon solar cells with reduced temperature sensitivity. Electron. Lett. 18, 97–98.

Hishikawa, Y., Doi, T., Higa, M., Yamagoe, K., Ohshima, H., Takenouchi, T., Yoshita, M., 2018. Voltage-dependent temperature coefficient of the I-V curves of crystalline silicon photovoltaic modules. IEEE J. Photovolt. 8, 48–53. https://doi.org/10.1109/JPHOTOV.2017.2766529.

IEC 60891, 2009. International Standard IEC 60891 - Photovoltaic devices - Procedures for temperature and irradiance corrections to measured I-V characteristics, 2.0. ed. International Electrotechnical Commission (IEC), Geneva.

Ishaque, K., Salam, Z., Taheri, H., 2011. Simple, fast and accurate two-diode model for photovoltaic modules. Sol. Energy Mater. Sol. Cells 95, 586–594. https://doi.org/10.1016/j.solmat.2010.09.023.

Lo Brano, V., Orioli, A., Ciulla, G., Di Gangi, A., 2010. An improved five-parameter model for photovoltaic modules. Sol. Energy Mater. Sol. Cells 94, 1358–1370. https://doi.org/10.1016/j.solmat.2010.04.003.

Orioli, A., Di Gangi, A., 2013. A procedure to calculate the five-parameter model of crystalline silicon photovoltaic modules on the basis of the tabular performance data. Appl. Energy 102, 1160–1177. https://doi.org/10.1016/j.apenergy.2012.06.036.

Osterwald, C.R., Glatfelter, T., Burdick, J., 1987. Comparison of the Temperature Coefficients of the Basic I-V Parameters for Various Types of Solar Cells. Conf. Rec. IEEE Photovolt. Spec. Conf. 188–193.

Paudyal, B.R., Imenes, A.G., 2021. Investigation of temperature coefficients of PV modules through field measured data. Sol. Energy 224, 425–439. https://doi.org/10.1016/j.solener.2021.06.013.

Piccoli Junior, A.L., Winck, A.L., Krenzinger, A., 2020. Determinação Da Variação Espectral Da Irradiância Na Substituição Das Lâmpadas De Um Simulador Solar, in: VIII Congresso Brasileiro de Energia Solar – Fortaleza, 01 a 05 de Junho de 2020.

Skoplaki, E., Palyvos, J.A., 2009. On the temperature dependence of photovoltaic module electrical performance: A review of efficiency/power correlations. Sol. Energy 83, 614–624. https://doi.org/10.1016/j.solener.2008.10.008.

Villalva, M.G., Gazoli, J.R., Filho, E.R., 2009. Comprehensive approach to modeling and simulation of photovoltaic arrays. IEEE Trans. Power Electron. 24, 1198–1208. https://doi.org/10.1109/TPEL.2009.2013862.